International Journal of Architectural, Civil and Construction Sciences
ISSN: 2415-1734
Vol:10, No:11, 2016

Performance Analysis of Air-Tunnel Heat Exchanger Integrated into Raft Foundation

Chien-Yeh Hsu, Yuan-Ching Chiang, Zi-Jie Chien, Sih-Li Chen

***Abstract*—**In this study, a field experiment and performance analysis of air-tunnel heat exchanger integrated with water-filled raft foundation of residential building were performed. In order to obtain better performance, conventional applications of air-tunnel inevitably have high initial cost or issues about insufficient installation space. To improve the feasibility of air tunnel heat exchanger in high-density housing, an integrated system consisting of air pipes immersed in the water-filled raft foundation was presented, taking advantage of immense amount of water and relatively stable temperature in raft foundation of building. The foundation-integrated air tunnel was applied to a residential building located in Yilan, Taiwan, and its thermal performance was measured in the field experiment. The results indicated that the cooling potential of integrated system was close to the potential of soil-based EAHE at 2 m depth or deeper. An analytical model based on thermal resistance method was validated by measurement results, and was used to carry out the dimensioning of foundation-integrated air tunnel. The discrepancies between calculated value and measured data were less than 2.7%. In addition, the return-on-investment with regard to thermal performance and economics of the application was evaluated. Because the installation for air tunnel is scheduled in the building foundation construction, the utilization of integrated system spends less construction cost compare to the conventional earth-air tunnel.

***Keywords*—**Air tunnel, ground heat exchanger, raft foundation, residential building.

I. Introduction

IN the past decade, air tunnel heat exchanger had attracted much attention of investigators and researchers that worked on studies of building energy conservation. The use of air tunnel heat exchanger combined with other passive cooling techniques may not only satisfy thermal comfort requirements of different types of occupants but reduce the energy consumption of indoor thermal environmental control. Buried under ground and surrounded by soil, conventional air tunnel heat exchanger in most cases is referred to as earth-air heat exchanger (EAHE) or soil-air heat exchanger. In order to achieve better thermal transfer or higher temperature difference of the tunnel system, the heat transfer sections of the tunnel system often need to be buried beneath the ground surface over 2 m depth where the soil temperature is less affected by surface thermal conditions, namely ground surface treatments (vegetation, cover of concrete, canopy, or even bare land) and ambient temperature. Furthermore, if the air tunnels are not designed right under the building structure, the designer must find other available space around the building to set those tunnels. Also, the soil type and moisture content, relating to the thermal diffusivity of heat transfer media, directly link to the underground soil temperature that strongly influents the air temperature within the tunnels. In general, there are too many design factors dominate the final thermal efficiency of EAHE. One or more constraints of design factors in each case of EAHE application inevitably cause high initial cost, problem of installation space or insufficient efficiency of the tunnel system. Many researchers [1]-[6] suggested that utilization of building structure such as foundation can be an option to construct a ground heat exchanger in a way of minimum initial cost. Several studies [1]-[8] provided systems which utilize the building structure as close loop ground heat exchanger combined with heat pump, but there is still lack of investigation in combination of building structure and the air tunnel system.

The combination of deep foundation piles and water pipe heat exchangers is often considered to be energy pile system. This deep foundation application will not be discussed here, but rather we will focus on the 'shallow foundation' structure. The 'shallow foundation' transfers building loads to the earth very near the surface, rather than to a range of depths as does a deep foundation. For adequate earthquake resistance, high residential building designers in Taiwan recently started to focus on the use of raft foundation, one kind of shallow foundation, that bears a load over its whole surface and is a structure spreading the seismic force to the ground. Because of its raft-like configuration, the raft foundation provides many void space, where commonly be backfilled with relatively expensive soil or just be remained empty. Cheng et al. [9] proposed an idea for urban water conservation by using abundant idle raft foundation of existing buildings. The idea has been verified by a case study. The objective of the case study is a 12-stories building located in Taipei City with two-level basement and a total of 82 apartments unit. The study concluded that according to survey and statistical analysis, a total water store capacity of exiting building raft foundations in Taipei city is approximately 9.8 million cubic meters. Gustafsson et al. [10], [11] has conducted several experiments to measure the natural convection improvement in water-filled borehole heat exchanger. The water-filled borehole means that the U pipes for heat transfer is almost immersed in groundwater

Chien-Yeh Hsu is with the Department of Mechanical Engineering, National Taiwan University, No. 1, Sec. 4, Roosevelt Road, Taipei, 106 Taiwan (phone: 886-2-33664497, fax: 886-2-23631808; e-mail: d00522028@ntu.edu.tw).

Yuan-Ching Chiang is with the Department of Mechanical Engineering, Chinese Culture University, 11114, Taiwan (e-mail: jyj3@ulive.pccu.edu.tw).

Zi-Jie Chien is with the Department of Mechanical Engineering, National Taiwan University, No. 1, Sec. 4, Roosevelt Road, Taipei, 106 Taiwan (e-mail: zijie80@gmail.com).

Sih-Li Chen is with the Department of Mechanical Engineering, National Taiwan University, No. 1, Sec. 4, Roosevelt Road, Taipei, 106 Taiwan (phone: 886-2-23631808, fax: 886-2-23631808; e-mail: slchen01@ntu.edu.tw).

then surrounding by soil. They summarized that because of the convection-based heat exchanger configuration, convective flow results in a 2-4 times more effective heat transfer through the borehole than pure conductive heat transfer. That is to say, we can also replace the soil conduction by apply the natural convection (or even forced convection) to improve the efficiency of air tunnel system. Moreover, Nam and Chae [12] explained that the annual temperature fluctuation of raft (or mat) foundation, installed at a depth of -3 to -10 m under the ground, is relatively stable, even though this zone is influenced by the heat flux of ground surface.

In this study, we take advantage of the immense amount of water and relatively stable temperature in raft foundation, immersing the air tunnel in the water reservoir of the foundation, to practice the foundation-integrated air-tunnel heat exchanger (FAHE). The FAHE can be an appropriate design when it is difficult to find an additional unused land in urban area for installation of air tunnel system. A field experiment and a performance analysis method based on thermal resistance method were performed. The thermal performance of the FAHE applied to the foundation of a residential building was measured in the field experiment.

II. Outline of Case Study

Fig. 1 illustrates the conceptual diagram of the object of case study which is a three-stories residential building located in Yilan County, Taiwan. Because of the experimental purposes and the measuring of thermal performance, a machine room dedicated to monitoring apparatus and HVAC system consists of chillers, air handling unit, air supply ducts and registers, is included in the building design. To provide indoor air ventilation for entire building, the FAHE connected with air handling unit has been installed.

The FAHE is similar to the conventional EAHE, generally consisting of a series of metallic or plastic pipes buried under the building through which the outdoor ambient air flows. However, the pipes so called air tunnels are settled in the water of raft foundation instead of solid soil. Fig. 2 shows the schematic plan view of the raft foundation of object building and the locations of temperature measuring points for each reservoir. The raft foundation which is about 22 m in length, 6.4 m in width, and 1.3 m in height, is divided into 7 parts by the shear walls of foundation, and each part is utilized as water reservoir except the first part, which is used as basement for experimental purposes. A photographic view of the experimental set-up of foundation and air tunnels can be seen in Fig. 3. As shown in Fig. 3, there are connecting pipes on each shear wall of raft foundation so that water can freely flow among reservoir 2 to 6. Four polyvinyl chloride pipes used as air tunnels presented in this study all pass through the shear walls of foundation from reservoir 2 to reservoir 4, taking a U-turn at reservoir 4, and continue going from reservoir 4 to reservoir 6, finally connected to the air handling unit in the machine room. The pipes immersed in the water of reservoirs have average length of 40 m with 0.2 m inside diameter. The specifications of EAHE pipes are listed in Table I. Each pipe is laid below water level at a gradient of 0.3 m to 0.05 m to allow the system to drain properly. For the safety of building construction, we have made rigorous check to ensure the installation of air tunnel through the foundation shear walls will not weaken the strength of the raft foundation.

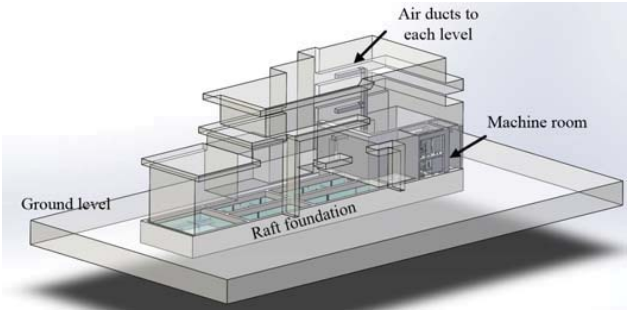

Fig. 1 Conceptual diagram of the object of case study

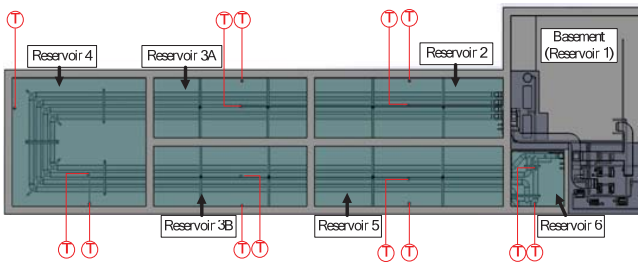

Fig. 2 Conceptual diagram of the object of case study

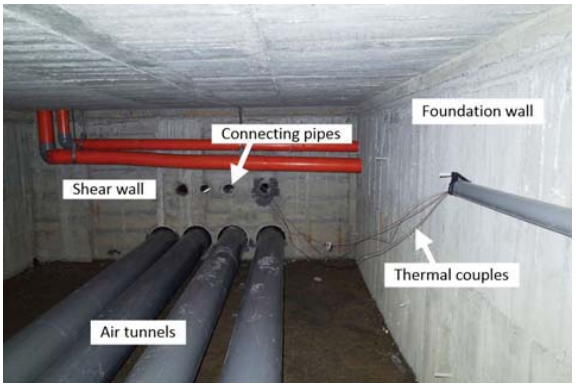

Fig. 3 Photographic view inside the raft foundation

To monitor the thermal condition of the entire water region of raft foundation, the temperature of foundation wall and outer surface of air tunnel pipe are measured. The detailed measurement items and equipment are listed in Table II.

TABLE I
Specification of Pipes in Raft Foundation

Material	PVC
Inner diameter (m)	0.202
Outer diameter (m)	0.216
Average length (m)	40
Number of pipes	4

TABLE II
MEASUREMENT ITEMS

Items	Sensor type	Purpose/Locations	Accuracy
Temperature	T-type thermal couple	Water, soil and airflow temperature measurement, locations of water measuring see Fig. 2	±0.5 ℃
Electricity consumption	Watt-hour meter	Power consumption of fan	±1%
Airflow velocity	Hot wire anemometer	Circulating airflow rate measurement, located at the inlet of EAHE	±2%
Air humidity	Wet bulb temperature sensor (thermal couple based)	Airflow humidity measurement, located at the inlet and outlet of EAHE	±0.5 ℃

III. PERFORMANCE ANALYSIS

A. Simplified Thermal Analysis

In the thermal analysis, a lumped system is utilized to simplify the mathematical model. The following assumptions are made for simplification:

1) One-dimensional heat transfer is considered, so that the effect of geometric design for the raft foundation is not account for.
2) In the reservoir of foundation, the time-dependent variable includes only the temperature of water that is spatially uniform at any instant during the transient process.
3) The airflow temperature at inlet of the air tunnel is defined as constant in each given time interval.
4) Heat generation, radiation effects and heat losses from the air tunnel and foundation walls are neglected.
5) Physical properties of fluids and materials are constant.

Based on the principle of energy conservation, the energy balance for a water-immersed air tunnel system is expressed by:

$$\frac{dE}{dt} = \dot{E}_{in} - \dot{E}_{out} = M_w C_{p,w} \frac{dT_w}{dt} \tag{1}$$

where dE/dt, $\dot{E}_{in}$, $\dot{E}_{out}$, M_w, $C_{p,w}$, and T_w are the rates of change in the total energy, the rate of energy entering and leaving the control volume, the mass of the water in foundation reservoir, the thermal capacity of the water, and the water temperature, respectively.

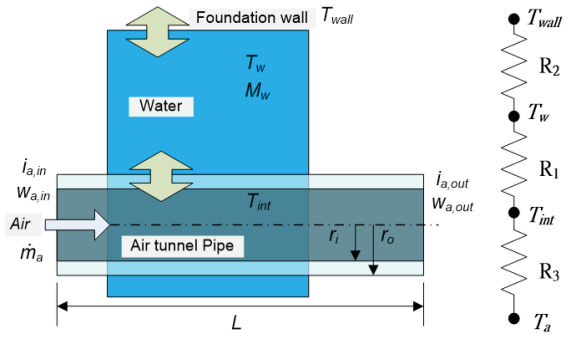

Fig. 4 Control volume and simplified thermal resistance of the foundation reservoir and the air tunnel

Fig. 4 presents the control volume surrounding the foundation reservoir and the air tunnel with cooling mode of air tunnel pipe. The direction of energy flow $\dot{E}_{in}$ and $\dot{E}_{out}$ may be reversed in heating mode. In cooling mode, the inlet air is being cooled by air tunnel. The rate of heat exchange between air tunnel and water is considered to be the rate of energy entering the control volume of water, which equals the enthalpy change of the air flow. By using the thermal resistance method, the passible amount of heat transfer can be estimated from the temperature of inner surface of pipe wall, T_{int}, and temperature of water, T_w, with total thermal resistance between inner surface of air tunnel and water, R_1:

$$\dot{E}_{in} = N\left(\frac{\dot{m}_a}{N}\Delta i_a\right) = N\left(\frac{T_{\text{int}} - T_w}{R_1}\right) \tag{2}$$

where $\dot{m}_a$ is the total mass flow rate of air, and Δi_a represent the enthalpy difference between inlet and outlet air, N is the number of pipes of air tunnel.

As the raft foundation is sealed, the heat can leave the control volume of water only in one way: Free convective cooling of the foundation walls. This exit method is expressed by

$$\dot{E}_{out} = \frac{T_w - T_{wall}}{R_2} \tag{3}$$

where T_{wall} is the temperature of foundation wall, R_2 is the total thermal resistance between the water and the foundation wall.

Because the energy can transfer across the pipe only by conduction, the temperature of air-pipe interface is the key to the total energy balance, and then the enthalpy difference of air stream due to energy transfer at the air-pipe interface inside the air tunnel can be expressed as:

$$\frac{\dot{m}_a}{N} di_a = h_c\left(T_a - T_{\text{int}}\right)\cdot 2\pi r_i dx \tag{4}$$

At first, for calculating the sensible heat change, ΔQ_c, it is necessary to know the thermal condition inside the air tunnel. For estimating the profile of temperature and humidity ratio, we follow an approximate method proposed by Cucumo et al. [13], which uses the following quadratic relations:

$$T^*(x) = T_a(x) - T_{\text{int}}(x) \tag{5}$$

$$T^*(x) = T^*(0) - \frac{T^*(0) - T^*(L)}{L}x + \frac{T^*(0) - T^*(L)}{L^2}x^2 \tag{6}$$

Because the temperature of inner pipe surface is considered to be constant along the entire length in this study, (5) and (6) can be reduced to:

$$T_a(x) - T_{\text{int}} = T_a(0) - T_{\text{int}} - 2\frac{T_a(0) - T_a(L)}{L}x + \frac{T_a(0) - T_a(L)}{L^2}x^2 \tag{7}$$

By using (7) and the fixed values of average temperature at the inlet $T_a(0)$ and outlet $T_a(L)$, the total amount of heat transfer due to finite temperature difference across the entire air tunnel can then be calculated:

$$\frac{\dot{m}_a}{N}\Delta i_a = \int_0^L h_c\left(T_a - T_{\text{int}}\right)\cdot 2\pi r_i dx = \frac{\overline{T}_a - T_{\text{int}}}{R_3} \tag{8}$$

with

$$R_3 = \frac{1}{2\pi r_i L h_c} \quad \text{and} \quad \overline{T}_a = \frac{T_a(0) + 2T_a(L)}{3} \tag{9}$$

When conducting the sizing process of heat exchanger design, both input and output condition of process fluid are given as fixed value and the geometry of heat exchanger needs to be determined. Therefore, the unknown factors remain the length of the air pipe *L* and the humidity ratio of the air at the outlet. By rearranging (8), the explicit form of the length of air pipe *L* is then:

$$L = \frac{\dot{m}_a \Delta i_a}{2\pi r_i h_c N\left(\overline{T}_a - T_{\text{int}}\right)} \tag{10}$$

The link between (2) and (8) can be used to determine the temperature of inner pipe surface T_{int}:

$$T_{\text{int}} = \frac{R_1\overline{T}_a + R_3 T_w}{R_1 + R_3} \tag{11}$$

In order to calculate T_{int}, one can use the initial water temperature $T_w(t_0)$ in any time interval, $[t_0, t_1]$, to substitute T_w in (11).

For calculating the enthalpy difference of moist air, Δi_a, it is necessary to calculate the moisture content of outlet air. The possible condensed or evaporated (if there is some kind of water film or droplet on the pipe wall) mass flow rate of water between air stream and pipe wall can be expressed as:

$$\dot{m}_a dw_a = h_m\left(w_{\text{int}} - w_a\right)\cdot 2\pi r_i dx \tag{12}$$

where w_{int} is the saturated humidity ratio of the air evaluated at the temperature of pipe wall T_{int}. As the temperature of inner pipe surface is fixed, the corresponding humidity ratio at the outlet of air tunnel due to the difference in the vapor concentration is then:

$$w_a(L) = w_{\text{int}} + \left(w_a(0) - w_{\text{int}}\right)e^{-\frac{2\pi r_i h_m}{\dot{m}_a}L} \tag{13}$$

with

$$h_m \cong \frac{h_c}{C_{p,a}} \tag{14}$$

For simplicity, the mass transfer coefficient h_m is obtained through the hypothesis proposed by Heyns [14], assuming that the Lewis factor, which is defined as $Le_f = h_c / C_{p,a} h_m$, is approximately equal to unity.

The temperature of water changes with time following the derivation of (1), (2), and (3). Given that the temperature of foundation wall and inner surface of pipe are known constant during any time interval, (1) becomes a first-order differential equation with constant coefficients, leading to the relation of temperature variation of water:

$$T_w(t) = a + (T_0 - a)e^{-bt} \tag{15}$$

with

$$a = \frac{NR_2 T_{\text{int}} + R_1 T_{wall}}{R_1 + NR_2} \quad \text{and} \quad b = \frac{R_1 + NR_2}{R_1 R_2}\cdot\frac{1}{M_w C_{p,w}} \tag{16}$$

where T_0 is the initial water temperature. The dimensioning results of air tunnel can be derived from the iterative solutions from (10) and (13), expressing *L* and W_{out}, respectively. In addition, by rearranging (10) with known exchanger length, the explicit expression of air temperature at the outlet of a heat exchanger can be determined, in order to estimate the performance of the RAHE system.

B. Wall Temperature of Reservoir

In general, the wall temperature of foundation is proportional to the temperature of surrounding soil and directly links to the heat flux due to the temperature difference between the wall and water. However, for simplification, the variations of wall temperature caused by heat exchange from water and the horizontal heat conduction are neglected. In a specific time interval, the average wall temperature can be estimated by calculation of mean value from following equation, which presents the underground soil temperature profile along different depths:

$$T_{wall} = \frac{1}{H_f}\int_0^{H_f} T_{soil}(t_0, z)dz \tag{17}$$

with

$$T_{soil}(t, z) = \theta_m + \left(\theta_{\max} - \theta_m\right)\cdot e^{-\delta}\cdot\cos\left(2\pi\frac{t}{t^*} - \delta\right) \tag{18}$$

$$\delta = z\sqrt{\frac{\pi}{\alpha t^*}} \tag{19}$$

where H_f, t^*, t_0, θ_m, $\theta_{\max}$, and α are the depth of foundation, the period of temperature oscillation, the start time of specific time interval, the average and maximum value of ground surface temperature, respectively.

C. Thermal Resistance

The method of thermal resistance is applied to simplify the mathematical model of the thermal analysis. R_1 in (2) is the thermal resistance between the inner surface of air tunnel and

the water, R_2 in (3) is the thermal resistance between the foundation wall and water, and R_3 (defined in (4)) which can be listed as:

$$R_1 = \frac{\ln\left(\frac{r_o}{r_i}\right)}{2\pi\lambda_p L} + \frac{1}{2\pi r_o L h_w} \quad (20)$$

$$R_2 = \frac{1}{A_{wall} h_{wall}} \quad (21)$$

$$R_3 = \frac{1}{2\pi r_i L h_c} \quad (22)$$

where h_w , h_{wall} , and h_c are the convective heat transfer coefficients; r_o and r_i are the outside and inside radius of air pipe (air tunnel); A_{wall} is the total surface areas of foundation walls involved in the convective heat transfer, λ_p is the thermal conductivity of the pipe of air tunnel, and L is the length of air pipe, respectively.

The values of the natural convective heat transfer coefficient h_w and h_{wall} can be derived using the empirical equations as:

$$Nu = \left\{0.825 + \frac{0.387 Ra^{1/6}}{\left[1+(0.492/\mathrm{Pr})^{9/16}\right]^{8/27}}\right\}^2 \text{ for vertical wall} \quad (23)$$

$$Nu = \left\{0.6 + \frac{0.387 Ra^{1/6}}{\left[1+(0.559/\mathrm{Pr})^{9/16}\right]^{8/27}}\right\}^2 \text{ for long horizontal cylinder,}$$

$$Ra \le 10^{12} \quad (24)$$

$$h_w = \frac{\lambda_w}{2r_o} Nu \quad (25)$$

$$h_{wall} = \frac{\lambda_w}{H} Nu \quad (26)$$

where Nu is the Nusselt number, Ra is Rayleigh number, Pr is Prandtl number, λ_w is thermal conductivity of water, and H is the height of water level.

IV. Results

A. Measuring Results of Water

The long-term measurements of temperature, which have started in March 29th, 2016, provided general insights of the ambient environmental condition and temperature variation inside the water reservoir beneath the ground. Fig. 5 shows the transient distribution of air temperature in the outside region of the residential building and the water temperature, with sampling period from March 29th until April 16th in 2016. The temperature magnitude of ambient air varied between values of 15.5 °C and 32.5 °C. The temperature variations of each specific monitored reservoir are compared with the variation of external air temperature, in order to reach the purpose of the study that is to circulate this air through the immersed ducts to exchange heat with the water. The comparison indicates that the higher water potential for cooling than for heating the outdoor air even during relatively cold season under the climate condition in Taiwan. In addition, different locations of reservoirs have distinct cooling potential.

Fig. 6 summarizes the sorted data of percentage durations of temperature difference between ambient air and each reservoir, which represents the possible cooling/heating potential of water reservoirs of raft foundation during the period of measurement (432 hours). By defining 2°C temperature difference as the lower bound of cooling set point, the distinct value of cooling potential can be clearly stated. It can be seen from this figure that the reservoir 5 and 6 have about 50% cooling potential as the reservoir 4 and 3B have about 40% cooling potential. The design of housing orientation may lead to these differences because of the direct sunlight toward the outside bare land of reservoir 4.

The data from sorted temperature difference between ambient air and soil will be used here to conduct the comparison between FAHE and EAHE. The data from the same month of FAHE is screened out from the measuring data of soil-based EAHE provided by the continued work of Yu et al. [15]. Fig. 7 shows the selected data of 505 hours that may provide the similar weather condition respect with the FAHE data. According to the figure, the acceptable cooling potential is 36.4% to 50%, which is similar to the cooling potential trend of FAHE, 38% to 52%. Hence, the temperature of water in the foundation with 1.3 m depth may provide the same level of cooling ability compare to the temperature of soil at 3-4 m depth.

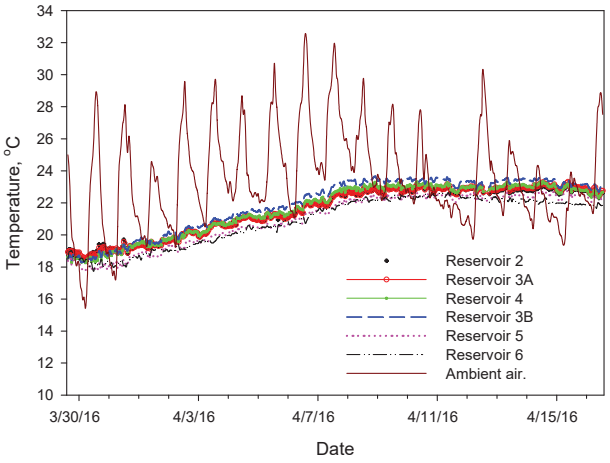

Fig. 5 Transient temperature variation of water in raft foundation and ambient air

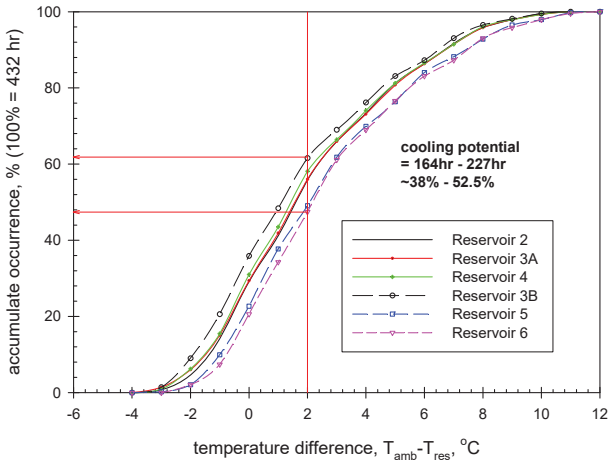

Fig. 6 Percentage occurrence of temperature difference between ambient air and water of each reservoir

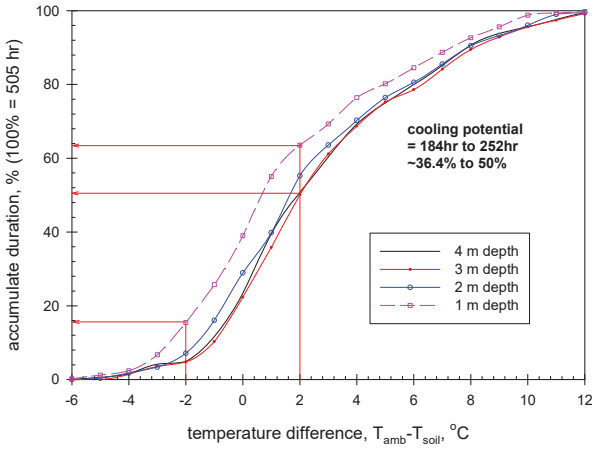

Fig. 7 Sorted temperature difference between ambient air and soil, with 505 hour selected data

B. Operating Performance of FAHE

In the present study, monthly continuing or intermittent operation of the fan was not available for operating test due to practical reason. Therefore, the implement of operating test for the FAHE was carried out in some selected date. The airflow velocity was fixed during all the operating tests, and was measured of 1.26 m/s. The cross sectional area of the air inlet was 0.322 m^2, so the total airflow rate was 1460 m^3/hour, leading the air mass flow rate of 0.47 kg/s. Based on the water level and the structural parameters of raft foundation, the water mass in the foundation was 84200 kg.

Case A: Testing Date March 29th, 2016

This testing started from 17:00 March 29th until 24:00 March 30th, representing a typical weather type during spring season in Taiwan. Fig. 8 depicts the 30 hours testing result of air temperature, humidity, and water temperature. As seen from the figure, the inlet air temperature varied between 15 °C and 23 °C along with the time, while the outlet temperature nearly closed to constant. The dew point temperature of inlet air, which also shown in the figure with continue line, was much lower than the both inlet and outlet temperature, leading the results that the humidity ratio did not change along with the EAHE pipe length. In addition, the air temperature perfectly damped to the temperature nearly equal to the mean water temperature of 18.5 °C in the raft foundation.

Case B: Testing Date May 26th, 2016

In Case B, the test started from 13:00 until 15:00 May 26th, representing a typical weather type during late spring season in Taiwan. In this season, the weather quickly became hot and humid. Fig. 9 shows the two hours testing results of thermal performance. The inlet air temperature decreased from 31 °C to 28.5 °C during the measurement period. The outlet air temperature, on the other hand, reached an almost steady state of 26 deg, about 1 °C above the mean water temperature. It is worth to notice that the water temperature was lower than dew point temperature at inlet. The humidity ratio at outlet was lower than that at inlet indicating that the wall temperature of pipes may lower than the dew point temperature and caused the moisture transfer. The average dehumidification rate was 1.84 kg/hour of water. The maximum and minimum enthalpy difference between inlet and outlet of air are 8.6 kJ/kg · K and 5 kJ/kg · K, leading the total heat transfer rate of 4 kW and 2.3 kW, respectively, with mass airflow rate of 0.47 kg/s. The mean heat transfer rate was 3.1 kW.

Case C: Testing Date May 31th, 2016

The test in the Case C started from 13:00 until 15:00 May 31th. This test was carried out in two days after the Case B, thus the water temperature data can be used to identify the change rate of temperature variation. The thermal performance results are collected in Fig. 10, which showed that the water temperature increased from 25 °C in Case B, to 26 °C in only two days' period. The housing orientation may lead to the direct sunlight toward the outside bare land of reservoir 4, causing the water temperature increase rapidly in some area. Except the inlet air temperature, the other parameters are nearly constant during the experimental study. Nonetheless, it can be known from the figure that the mean water temperature was almost equal to the dew point temperature at inlet, and can reach the dew point to affect the moisture mass transfer. The humidity ratio slightly declined of 0.001 kg_w/kg_a, indicating that the wall temperature of inner pipes was also below the dew point. The average dehumidification rate was 2.58 kg/hour of water. The maximum and minimum enthalpy difference between inlet and outlet of air are 10.3 kJ/kg · K and 5.6 kJ/kg · K, leading the total heat transfer rate of 4.84 kW and 2.6 kW, respectively, with mass airflow rate of 0.47 kg/s. The mean heat transfer rate was 3.66 kW.

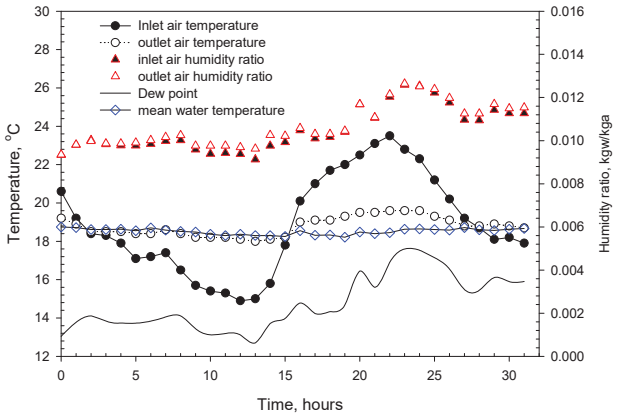

Fig. 8 Operating performance of FAHE, from 17:00 March 29th until 24:00 March 30th

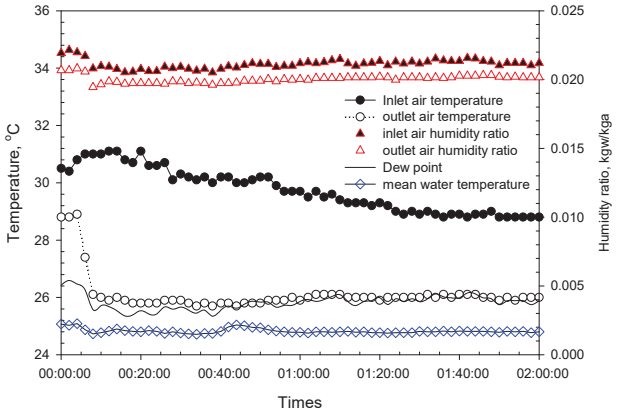

Fig. 9 Operating performance of FAHE, from 13:00 until 15:00, May 26th

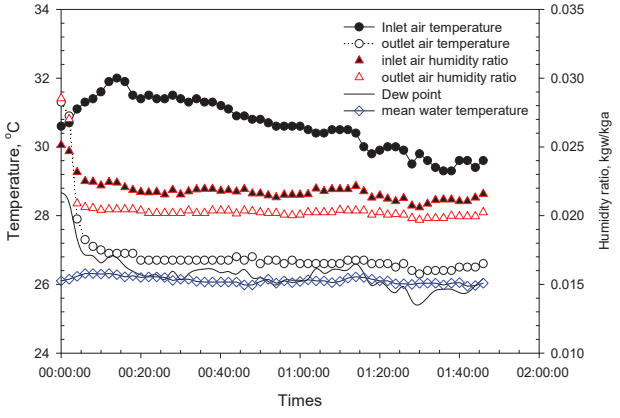

Fig. 10 Operating performance of FAHE, from 13:00 until 15:00, May 31th

C. Validation of Analytical Model

The analytical model was validated by using the in-situ experimental data, in order to calibrate the model for developing easy-to-use dimensioning tool. Figs. 11 and 12 present the comparison using the data from Case A and Case B, respectively. The simulated outlet temperature shows a good agreement with the experimental data. All predicted values are in the range of ±2.3 °C relative error compared to Case A and in the range of ±2.7 °C relative error compared to Case B.

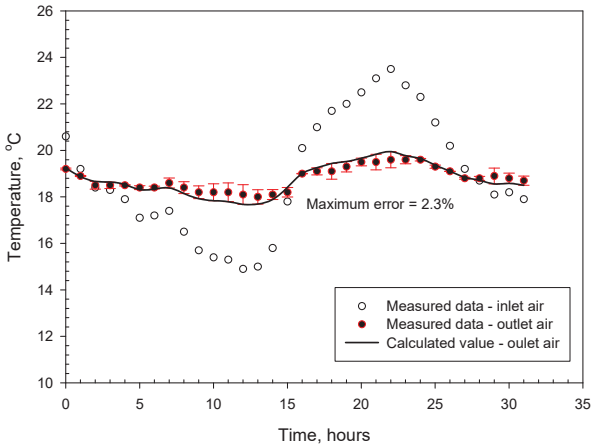

Fig. 11 Comparison between measured and calculated temperature of outlet air with same inputs from Case A

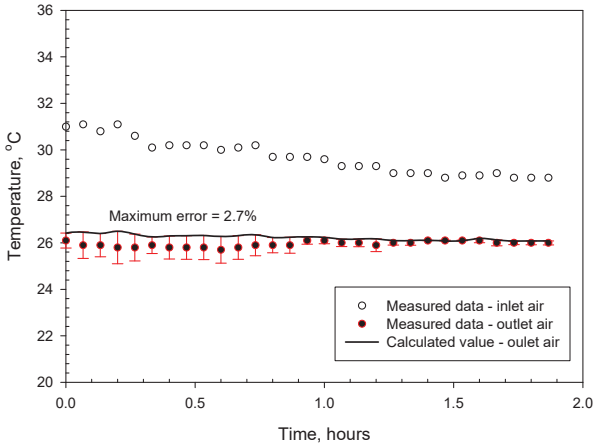

Fig. 12 Comparison between measured and calculated temperature of outlet air with same inputs from Case B

D. Dimensioning Calculation for Case B

In general, one faces the dimensioning (or sizing) issue while a heat exchanger may need to be designed specifically for requirements including special characteristics. In fact, the structural factors (e.g., pipe length) of the FAHE constructed for the in-situ experiment was not optimized. The length of pipes was mainly depended on the structural of the raft foundation. Thus, the analytical model can be used to provide the solution for the sizing issue of FAHE. Fig. 13 presents effect of pipe length on both the outlet temperature and total heat transfer rate based on the conditions of Case B. The results indicate that the change rate of outlet temperature along with the length of pipe is near 0.04 °C/m around the length of 40 m, and it continues declining when the length increases. Decreasing 10 m length for a case of FAHE with 40 m length could lead only 0.4 °C outlet temperature increased, with 400

W decline of heat transfer rate. If the pipe length was selected at 30 m, the heating capacity can be determined by rating design. The results of rating for average heating capacity was 1.2 kW during the period of 15 °C average ambient temperature. If the size or geometric of the FAHE can be freely determined by the result of dimensioning approach, the construction cost of FAHE can then be reduced with acceptable thermal performance output.

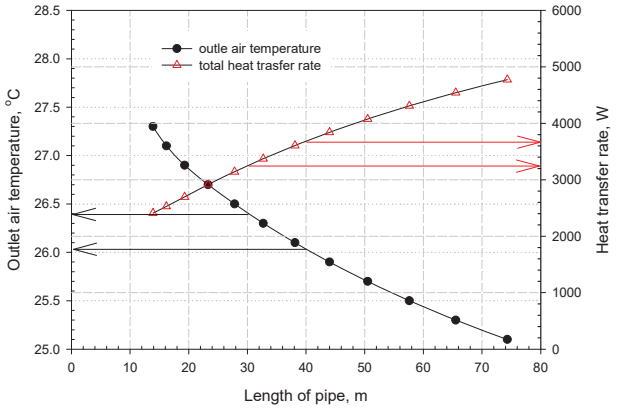

Fig. 13 Dimensioning result of the FHAE, based on Case B

E. Economic Aspect

The intent of developing the FAHE is to reduce the total costs compared with conventional EAHE. The capital costs and return on investment (ROI) can be a reference for future application. The capital costs of the FAHE system are divided into initial investment, including installation, and operating costs for system operation and maintenance.

The initial cost of FAHE system can vary dramatically, mainly depending on the construction cost. The total construction costs may include pipe setup, payroll expenses, personnel expenses, and supplies expenses. In order to have better understanding of the ROI for FAHE systems, a baseline case is introduced. The baseline case is considering a new designed building that is going to use a 10RT chiller for air conditioning and 5 kW electric heater for air heating, without any air pretreatment. The 10 RT chiller is considered to have costs of US$ 5000 for chiller equipment and costs of US$ 300 for system setup. The 5 kW electric air heater is estimated to have costs of US$ 600. Based on the dimensioning design, the length of air ducts was selected to have 30 m length with 3.21 kW average cooling capacity. Therefore, the Air ducts, which is estimated at 19 US$/m, will cost US$ 2280 with total length of 120 m (four 30 m pipe). The drainage system for pipe cleaning and condensate-free is valued at US$100 for FAHE. The fan may have US$ 150 on costs to drive sufficient airflow. The excavate-cost-free is the main advantage of the FAHE thus the total initial cost of FAHE is slightly lower than that of conventional EAHE.

Using the experiment data and the further case study, the heat transfer rate was selected to have 3.21 kW cooling capacity with 30 m length at noon during spring and summer season. This daily average heat transfer can be achieved if the midday intermittent operating control is available. The power consumption of the fan is 0.45 kW, so the COP of the FAHE is estimated at 7.1. Considering the chiller of baseline has a monthly average COP of 3, the 3.21 kW heat load from outside fresh air will consume 1.07 kW power from the chiller for cooling treatment. In addition, when chiller is working, the chilled water pump and the ventilation fan are also needed to start up. In general, the water pump and ventilation fan consume 1HP (0.746 kW) and 0.3 kW, respectively. Therefore, the total power consumption of chiller will become 2.116 kW.

Assuming that the cooling hour per day is 10, and 25 working days per month, the cooling operating duration will be 250 hours per month. The period of annual cooling is 7 months (from May until November), so that the annual cooling hours is 1750 hours/year. Besides, the annual heating demand is 500 hours/year (for 10 hours a day, 25 working days per month, and 2 months annual heating). The cost of power consumption is estimated at 0.2 US$/kWh. The annual operating costs of the baseline is 1241 US$/year, and the evaluation for the ROI period of FAHE is about 4 years. Using the EAHE can reduce to operating costs to 538 US$/year. The initial costs have huge effect on the ROI period, and an appropriate dimensioning of FAHE can significantly reduce the construction costs, lowering the initial costs. Therefore, the structural design will be the key point of the real application.

V. Conclusion

Efficient heat transfer media is one of the most important design consideration of air-tunnel heat exchanger. The results of investigation for FAHE concluded that the cooling potential of the water beneath a building of 1.3 m during spring season was close to that of ground soil at 2 m depth or deeper. The effect of changing the media around the air-tunnel is significant. However, there is still room for improvement of thermal potential of FAHE system. A suitable treatment of the ground surface is also important to avoid extra heat added into the water in the foundation. Therefore, the further research will focus on improving the performance of air-tunnel heat exchanger by circulating the foundation water with underground water or rainwater collection system to improve the thermal condition of foundation water.

Acknowledgment

The authors gratefully acknowledge the financial support provided by the Bureau of Energy, Ministry of Economic Affairs, Taiwan, R. O. C.

References

[1] J.-U. Lee, T. Kim, and S.-B. Leigh, “Applications of building-integrated coil-type ground-coupled heat exchangers—Comparison of performances of vertical and horizontal installations,” Energy and Buildings, vol. 93, pp. 99–109, 2015.
[2] Y. Hamada, H. Saitoh, M. Nakamura, H. Kubota, and K. Ochifuji, “Field performance of an energy pile system for space heating,” Energy and Buildings, vol. 39, no. 5, pp. 517–524, 2007.
[3] J. Gao, X. Zhang, J. Liu, K. S. Li, and J. Yang, “Thermal performance and ground temperature of vertical pile-foundation heat exchangers: A case study,” Applied Thermal Engineering, vol. 28, no. 17-18, pp. 2295–2304, 2008.

[4] D. Bozis, K. Papakostas, and N. Kyriakis, “On the evaluation of design parameters effects on the heat transfer efficiency of energy piles,” Energy and Buildings, vol. 43, no. 4, pp. 1020–1029, 2011.
[5] Jalaluddin, A. Miyara, K. Tsubaki, S. Inoue, and K. Yoshida, “Experimental study of several types of ground heat exchanger using a steel pile foundation,” Renewable Energy, vol. 36, no. 2, pp. 764–771, 2011.
[6] H. Park, S.-R. Lee, S. Yoon, and J.-C. Choi, “Evaluation of thermal response and performance of PHC energy pile: Field experiments and numerical simulation,” Applied Energy, vol. 103, pp. 12–24, 2013.
[7] J. Luo, H. Zhao, S. Gui, W. Xiang, J. Rohn, and P. Blum, "Thermo-economic analysis of four different types of ground heat exchangers in energy piles," Applied Thermal Engineering, vol. 108, pp. 11-19, 2016.
[8] K. Tsubaki and Y. Mitsutake, "Performance of ground-source heat exchangers using short residential foundation piles," Energy, vol. 14, pp. 229-236, 2016.
[9] C. Cheng, Y. Liu, and C. Ting, “An urban drought-prevention model using raft foundation and urban reservoir,” Building Services Engineering Research and Technology, vol. 30, no. 4, pp. 343–355, 2009.
[10] A.-M. Gustafsson, L. Westerlund, and G. Hellström, “CFD-modelling of natural convection in a groundwater-filled borehole heat exchanger,” Applied Thermal Engineering, vol. 30, no. 6-7, pp. 683–691, 2010.
[11] A.-M. Gustafsson and L. Westerlund, “Multi-injection rate thermal response test in groundwater filled borehole heat exchanger,” Renewable Energy, vol. 35, no. 5, pp. 1061–1070, 2010.
[12] Y. Nam and H.-B. Chae, “Numerical simulation for the optimum design of ground source heat pump system using building foundation as horizontal heat exchanger,” Energy, vol. 73, pp. 933–942, 2014.
[13] M. Cucumo, S. Cucumo, L. Montoro, and A. Vulcano, “A one-dimensional transient analytical model for earth-to-air heat exchangers, taking into account condensation phenomena and thermal perturbation from the upper free surface as well as around the buried pipes,” International Journal of Heat and Mass Transfer, vol. 51, no. 3-4, pp. 506–516, 2008.
[14] J.A. Heyns, D.G. Kröger, “Experimental investigation into the thermal-flow performance characteristics of an evaporative cooler,” Applied Thermal Engineering, vol. 30, pp. 492–498, 2010.
[15] P.-Y. Yu, H.-C. Hsu, Y.-C. Chang Y.-C. Chiang, C.-Y. Hsu and S.-L. Chen, “Energy-Saving Evaluation of a District Air Conditioning System Incorporated with Ground Heat Exchangers Used in an Employee's Cafeteria,” Proceedings of the 7th Asian Conference on Refrigeration and Air Conditioning, ACRA2014-319, 2014